



# Deep learning assessment of fetal brain maturation on 3D ultrasound volumes in early-onset fetal growth restriction

L. MEIJERINK<sup>1</sup> , M. WYBURD<sup>2</sup>, A. I. L. NAMBURETE<sup>2,3</sup>, T. ALDERLIESTEN<sup>4</sup>, F. GROENENDAAL<sup>4</sup>, M. BENDERS<sup>4</sup>, F. TERSTAPPEN<sup>1,4</sup> and M. N. BEKKER<sup>1</sup> 

<sup>1</sup>Department of Obstetrics, Division Woman & Baby, University Medical Center Utrecht, Utrecht University, Utrecht, The Netherlands; <sup>2</sup>Oxford Machine Learning in Neuroimaging Laboratory, Department of Computer Science, University of Oxford, Oxford, UK; <sup>3</sup>Oxford Centre for Integrative Neuroimaging, University of Oxford, Oxford, UK; <sup>4</sup>Department of Neonatology, Division Woman & Baby, University Medical Center Utrecht, Utrecht University, Utrecht, The Netherlands

**KEYWORDS:** deep-learning model; fetal brain maturation; fetal growth restriction

## ABSTRACT

**Objectives** To quantify fetal brain maturation in fetuses with early-onset fetal growth restriction (FGR) by estimating gestational age (GA) based on the appearance of gyrification and individual brain structures from three-dimensional (3D) ultrasound volumes using a deep-learning model trained on optimally developing subjects. The association of altered fetal brain maturation, as a potential marker of cumulative intrauterine stress, with an increased risk of neonatal complications was also explored.

**Methods** This was a prospective, observational, single-center cohort study of singleton pregnancies with early-onset FGR conducted at the University Medical Center Utrecht between June 2022 and June 2024. Early-onset FGR was defined as an estimated fetal weight (EFW) and/or abdominal circumference below the 10<sup>th</sup> percentile before 32 weeks' gestation, and brain sparing was defined as an umbilical artery pulsatility index (PI) above the 95<sup>th</sup> percentile in combination with a middle cerebral artery PI below the 5<sup>th</sup> percentile or a cerebroplacental ratio (CPR) < 1. Fetal brain maturation was determined using a deep-learning model, which was trained on data from an optimally developing cohort at GAs of between 18 + 0 and 28 + 6 weeks, collected by the INTERGROWTH-21<sup>st</sup> Consortium. Therefore, only fetuses with a GA of < 29.0 weeks at the time of the scan were included in the analysis. Estimation of brain maturation was based on the size and shape of the Sylvian fissure (SF), parieto-occipital fissure (POF) and calcarine sulcus (CLC), cerebellum (CB) and the combination of all fissures using the whole-brain ultrasound scan. The mean difference between estimated

GA and actual GA ( $\Delta$ GA) in days was calculated. In a subgroup analysis,  $\Delta$ GA for brain-sparing FGR was compared with  $\Delta$ GA for non-brain-sparing FGR. Regression analysis was performed to examine the relationship between brain maturation data and potential covariates.

**Results** The study included 43 growth-restricted fetuses with high-quality 3D ultrasound scans (13 of which had brain-sparing FGR) at a median GA of 27.1 (interquartile range (IQR), 26.1–27.7) weeks. The estimated GA was significantly lower than the actual GA in early-onset FGR, with  $\Delta$ GA of -4.6 (IQR, -9.8 to -1.0) days based on the whole scan,  $\Delta$ GA of -4.9 (IQR, -9.0 to -1.2) days based on the SF,  $\Delta$ GA of -5.4 (IQR, -7.4 to -1.7) days based on the POF and CLC, and  $\Delta$ GA of -3.2 (IQR, -6.8 to 0.3) days based on the CB ( $P < 0001$  for all). There was no significant difference in brain maturation between fetuses with brain-sparing and those with non-brain-sparing FGR or between male and female fetuses. The EFW percentile correlated significantly with the degree of delayed maturation (whole-scan data,  $r = 0.377$ ;  $P = 0.013$ ) and contributed to our multivariable model. Socioeconomic status, fetal sex and CPR were not associated with the delay in maturation. Seventeen neonates were born < 32.0 weeks' gestation and admitted to the neonatal intensive care unit. The  $\Delta$ GA was higher in the neonates with perinatal complications, indicating greater delay in brain maturation.

**Conclusions** Delayed fetal brain maturation in early-onset FGR has been demonstrated using a 3D ultrasound deep-learning model. These findings highlight the potential role of 3D ultrasound in the assessment of fetal brain maturation and support the

Correspondence: Prof. M. N. Bekker, Lundlaan 6, 3584 EA Utrecht, The Netherlands (e-mail: m.n.bekker-3@umcutrecht.nl)

Accepted: 28 November 2025

need for continued research into these findings and their long-term neurodevelopmental consequences in early-onset FGR. © 2026 The Author(s). *Ultrasound in Obstetrics & Gynecology* published by John Wiley & Sons Ltd on behalf of International Society of Ultrasound in Obstetrics and Gynecology.

## INTRODUCTION

Fetal growth restriction (FGR) due to placental insufficiency is a common complication of pregnancy worldwide, with early-onset FGR being particularly relevant in low- and middle-income countries<sup>1–5</sup>. With no treatment for FGR, clinical management relies on close fetal monitoring and often necessitates early delivery once fetal well-being is at risk<sup>4,6–8</sup>. Consequently, many FGR pregnancies culminate in preterm birth, compounding the deleterious effects of prematurity with those of growth restriction on the developing brain<sup>1,9</sup>. FGR is associated with impaired brain development, particularly in brain-sparing FGR<sup>1,2,10</sup>. Neuroimaging studies show that FGR neonates have smaller cortical volumes but disproportionately elevated maturation, suggesting accelerated gyrification<sup>11</sup>. This paradoxical finding raises the question of whether FGR alters the trajectory of cortical development and highlights the need for prenatal tools to objectively assess gyrification.

Cortical gyrification is a key indicator of fetal brain maturation<sup>12</sup>. Currently, it is assessed qualitatively on ultrasound, as no objective method is routinely available<sup>13,14</sup>. Abnormal gyrification has been linked to neurodevelopmental disorders and adverse outcomes<sup>15</sup>. Ultrasound markers of gyrification, such as Sylvian fissure (SF) depth and angle, can be measured to gauge cortical development<sup>13,16</sup>. The Pistorius grading system divides cortical folding into five categories according to gestational age (GA)<sup>13</sup>. Using this system, Businelli *et al.*<sup>14</sup> found gyrification to be unchanged or even accelerated in growth-restricted fetuses. A study of early-onset FGR revealed only a slight decrease in right SF depth<sup>17</sup>. However, manual assessment is subject to significant interobserver variability, limiting reliability.

Fetal magnetic resonance imaging (MRI) enables objective quantification of cortical folding by computing metrics such as the gyrification index, cortical surface area, sulcal organization and curvature<sup>18,19</sup>. Nonetheless, ultrasound remains the gold standard for prenatal brain assessment owing to its cost-effectiveness, non-invasiveness and accessibility<sup>13,20–23</sup>. To bridge the gap between the ultrasound practicality and objective analysis, Wyburd *et al.*<sup>15</sup> developed an automated deep-learning-based pipeline that estimates GA based on fissure morphology<sup>24,25</sup>.

Given the link between FGR and altered brain development, in this study we applied a deep-learning model to three-dimensional (3D) ultrasound volumes from early-onset FGR fetuses to quantify cortical maturation. We also explored whether altered maturation, as a potential marker of cumulative intrauterine stress, is associated with an increased risk of neonatal complications<sup>15</sup>.

## METHODS

### Study design and population

This prospective, observational, single-center cohort study was conducted between 1 June 2022 and 1 June 2024 at the University Medical Center Utrecht, Utrecht, The Netherlands (ethical approval reference: 21-552). The inclusion criterion was a singleton FGR pregnancy below 32 weeks' gestation. FGR was defined as an abdominal circumference (AC) and/or estimated fetal weight (EFW) below the 10<sup>th</sup> percentile according to GA using the Hadlock formula<sup>26</sup>. Brain sparing was defined as an umbilical artery (UA) pulsatility index (PI) above the 95<sup>th</sup> percentile in combination with a middle cerebral artery (MCA)-PI below the 5<sup>th</sup> percentile or a cerebroplacental ratio (CPR) below 1<sup>27</sup>. All patients underwent an advanced fetal ultrasound examination, including targeted neurosonography, based on the International Society of Ultrasound in Obstetrics and Gynecology (ISUOG) protocol, with 3D ultrasound examination of the developing fetal brain as part of standard care<sup>28,29</sup>. Exclusion criteria were fetal congenital abnormalities including structural brain abnormalities, genetic syndromes or infections. All participants gave written informed consent.

### Data acquisition

Ultrasound was performed transabdominally using a 3D convex probe on a Voluson E10 ultrasound machine (GE Healthcare, Zipf, Austria) by several highly trained sonographers. All the sonographers had completed dedicated training in fetal neurosonography and followed a standardized acquisition protocol based on ISUOG guidelines to minimize interoperator variability<sup>28,29</sup>. At least two axial volume sweeps were performed per patient, one in the transthalamic plane and one in the transcerebellar plane. If a patient received multiple 3D volume sweeps at different GAs, the data were aggregated to generate a single value for analysis.

### Data processing

The sweeps at <29 weeks were pseudonymized and exported as NRRD files before transferring the data to the Oxford Machine Learning in Neuroimaging Laboratory, Oxford University, Oxford, UK. Quality was assessed according to the image inclusion criteria used for the atlas construction of the INTERGROWTH-21<sup>st</sup> Consortium<sup>24,25</sup>. This meant an overall absence of maternal and fetal motion artifacts, a depiction of the full fetal head with minimal acoustic shadow and clear contrast between fluid-filled cavities and dense regions like the skull<sup>24</sup>. This quality analysis was done blinded to outcome, excluding files with insufficient quality before debinding.

### Data analysis

To predict brain maturation, a deep-learning model developed by Wyburd *et al.*<sup>15</sup> was used. In brief, a 3D

ultrasound brain volume is input into the model and the model predicts the GA of that subject based on the appearance of the brain. The underlying methodology is not exclusive to 3D ultrasound and may be adapted for two-dimensional (2D) scans, however, the complex 3D morphology of fetal brain fissures and structures makes 2D imaging more dependent on the consistent acquisition of specific standard planes, with variation in fissure appearance across slices, potentially reducing algorithm robustness. 3D ultrasound was therefore selected to capture and model the full morphological information of these structures. The model was trained and five-fold cross-validated using data collected as part of the INTERGROWTH-21<sup>st</sup> Consortium Fetal Growth and Longitudinal Study. This dataset consists of ultrasound scans of optimally developing subjects, with normal long-term follow-up from eight international centers, and has been used to generate international growth standards<sup>30</sup>. As this model was trained on optimally developing subjects, the estimated GA can be used to assess brain maturation, and the mean difference between estimated GA and actual GA ( $\Delta$ GA) can be interpreted as a deviation from expected development.

Variations of the model were trained to base the maturation estimation on the appearance of: (1) SF; (2) parieto-occipital fissure (POF) and calcarine sulcus (CLC); (3) cerebellum (CB); and (4) the combination of all fissures using the whole-brain ultrasound scan. This pipeline has been validated for GAs between 18 + 0 and 28 + 6 weeks, therefore only scans obtained before 29 weeks were included in the analysis. It is important to note that in this pipeline, before GA prediction, the volumes are resampled to an isotropic voxel size of 0.6 mm using trilinear interpolation, before being aligned to a common reference space using the Brain Extraction and Alignment Network (BEAN) algorithm<sup>31</sup>. In BEAN, a scaling factor is learned and each image is scaled (or down-sampled) to match a reference total brain volume (TBV) based on the ultrasound atlas at 25 gestational weeks<sup>15</sup>. The scaling factor was applied using trilinear interpolation, so that all the volumes were approximately the same size. This ensures that the model is predicting brain maturation based on the appearance, texture and shape of structures and not just their size, which is driving change over this 10-week window.

Main outcomes included  $\Delta$ GA, based on SF, POF and CLC, CB and whole fetal brain morphology.

### Statistical analysis

Data were analyzed using IBM SPSS Statistics version 27.0 (IBM Corp., Armonk, NY, USA), and the linear regression models and graphs were generated using RStudio version 4.4.0 (R Foundation of Statistical Computing, Vienna, Austria)<sup>32,33</sup>. All data were tested for normality using the Shapiro–Wilk test<sup>34</sup>. The baseline characteristics are reported as mean  $\pm$  SD for normally distributed continuous data, and an independent student's *t*-test was used to compare brain-sparing FGR with

non-brain-sparing FGR. Non-normally distributed data were compared using the Mann–Whitney *U*-test and are reported as median (interquartile range (IQR)). Categorical dichotomous information is presented as *n* (%) and was analyzed using the Fisher's exact test or chi-square test, as appropriate.

The estimated GA was compared with the actual GA at the time of the ultrasound scan using the Wilcoxon signed-rank test. The  $\Delta$ GA was compared for brain-sparing and non-brain-sparing FGR and per fetal sex. The same was done for neonatal outcomes. Neonatal outcomes included perinatal death, admission to the neonatal intensive care unit (NICU) according to national protocol<sup>35</sup>, combined neonatal morbidity and mortality and neurological or respiratory complications. Neurological complications included the following imaging abnormalities: perinatal asphyxia, any degree of intraventricular hemorrhage, posthemorrhagic ventricular dilation, cystic periventricular leukomalacia and stroke. These represent radiological findings rather than functional performance, which was not assessed in this study. Respiratory complications included the need for mechanical ventilation, infant respiratory distress syndrome and bronchopulmonary dysplasia<sup>36</sup>.

Furthermore,  $\Delta$ GA was plotted cross-sectionally over actual GA in days. Correlation was evaluated using Pearson correlation or Spearman's rank test depending on the normality of the data. The correlation between  $\Delta$ GA and biometric and Doppler measurements for the severity of FGR, AC and EFW percentiles and brain sparing (UA-PI, MCA-PI, CPR) was assessed. We also examined the correlation of estimated GA with TBV.

Linear regression was performed with  $\Delta$ GA as the dependent variable, using backward selection based on the Akaike Information Criterion to refine the model and examine the relationship between the estimation of brain age and potential covariates. Covariates included in the analysis were GA at ultrasound, fetal sex, EFW percentile, CPR and socioeconomic status (SES), since the latter is a known risk factor for neurological impairment<sup>37</sup>. SES score was based on the 'welvaart, opleiding en arbeidsverleden' (WOA) score, which measures average income, education level and employment status of households for a given zip code. The average SES-WOA score is 0, and higher scores imply higher SES<sup>38,39</sup>. For neonatal data, logistic regression on binary outcomes was performed with and without the addition of  $\Delta$ GA based on whole-scan data. ANOVA was performed to determine whether the addition of the maturation data improved the model. Two-sided *P* < 0.05 was considered statistically significant.

## RESULTS

### Participant inclusion in study

Using the deep-learning model, brain maturation was estimated for 55 FGR patients at < 29 weeks' gestation (Figure 1). After blinded quality selection, 49 volume files

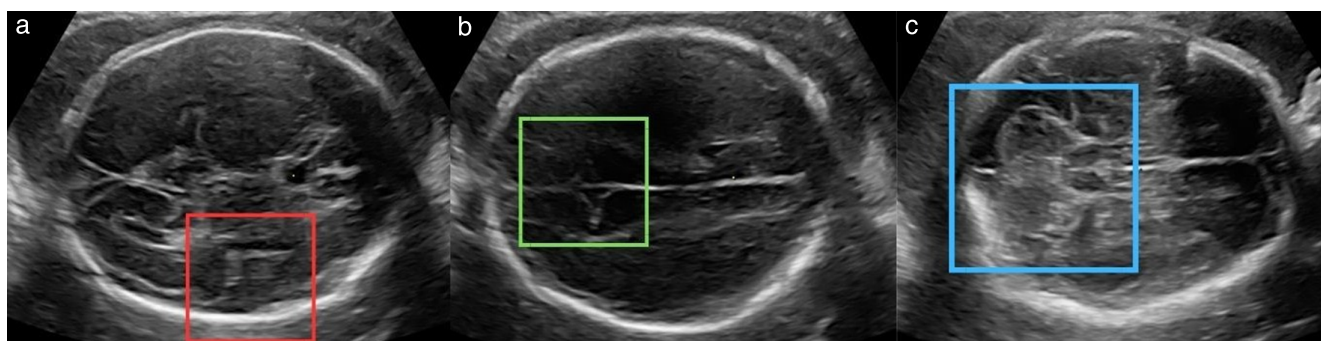


**Figure 1** Axial three-dimensional ultrasound images showing brain at 202 days' gestation in a growth-restricted fetus. Boxes indicate: (a) Sylvian fissure (estimated gestational age (GA), 193 days (mean difference between estimated and actual GA ( $\Delta$ GA), -9 days)), (b) parieto-occipital fissure and calcarine sulcus (estimated GA, 192 days ( $\Delta$ GA, -10 days)) and (c) cerebellum (estimated GA, 194 days ( $\Delta$ GA, -8 days)).

for 43 patients were included in the analysis. Four patients had two high-quality volume files at different GAs and one patient had three files. For these patients, the data were averaged per patient, resulting in 43 unique patients. The definition of brain-sparing FGR was met in 13 patients. One fetus developed brain sparing between two 3D ultrasound examinations and was therefore excluded for the comparison between brain-sparing and non-brain-sparing FGR. The median GA at the time of the ultrasound scan was 27.1 (IQR, 26.1–27.7) weeks. Corticosteroids for fetal lung maturation were administered in 15 patients, including 10 (76.9%) in the brain-sparing FGR group and five (17.2%) in the non-brain-sparing FGR group. All had normal ductus venosus flow at the time of administration. The clinical indications for corticosteroid use were as follows: five cases had normal UA Doppler, but corticosteroids were administered for maternal indication; two cases had UA-PI > 95<sup>th</sup> percentile with normal MCA-PI; three cases had UA-PI > 95<sup>th</sup> percentile in combination with brain sparing; four cases had absent end-diastolic flow; and one case had reversed end-diastolic flow. The median interval between corticosteroid administration and birth was 31 days. Further baseline characteristics are shown in Table 1.

### Prediction of fetal brain maturation

Estimated GA based on the 3D ultrasound-based deep-learning model was significantly lower than the actual GA of fetuses with FGR:  $\Delta$ GA, -4.6 (IQR, -9.8 to -1.0) days based on the whole scan,  $\Delta$ GA, -4.9 (IQR, -9.0 to -1.2) days based on the SF,  $\Delta$ GA, -5.4 (IQR, -7.4 to -1.7) days based on the POF and CLC and  $\Delta$ GA, -3.2 (IQR, -6.8 to 0.3) days based on the cerebellum ( $P < 0.001$  for all) (Table 2). When comparing the estimated and actual GA, there was no difference in brain maturation between fetuses with brain-sparing and those with non-brain-sparing FGR or between male and female fetuses (Tables 2 and S1). The distribution of fetal sex differed significantly between the brain-sparing and non-brain-sparing FGR groups, with females representing 30.8% and 75.9%, respectively ( $P = 0.01$ ). Therefore, an

interaction term between sex and CPR was included in the linear regression models. Furthermore, when plotting  $\Delta$ GA cross-sectionally over time, the maturation delay increased progressively with advancing GA (Figure 2).

### Correlation between delayed brain maturation and severity of FGR

The  $\Delta$ GA correlated positively with EFW percentile, thus the more severe FGR with lower EFW percentiles, the more delayed the brain maturation ( $\Delta$ GA based on: SF,  $r = 0.456$ ,  $P = 0.002$ ; POF and CLC,  $r = 0.370$ ,  $P = 0.015$ ; CB,  $r = 0.357$ ,  $P = 0.019$ ; and whole scan,  $r = 0.377$ ,  $P = 0.013$ ). The AC percentile correlated positively with  $\Delta$ GA based on the SF and the whole scan only ( $r = 0.294$ ,  $P = 0.056$  and  $r = 0.270$ ,  $P = 0.080$ , respectively). The UA-PI and CPR showed no correlation with the delay in brain maturation. In a linear model, estimated GA based on the whole-brain volume was associated significantly with TBV (adjusted  $R^2 = 0.75$ ,  $P < 0.001$ ) and TBV<sup>2</sup> (adjusted  $R^2 = 0.62$ ,  $P < 0.001$ ) (Figure S1).

### Linear regression analysis of delayed brain maturation

For the  $\Delta$ GA based on the whole scan, the final model included GA at ultrasound, EFW percentile and CPR, although only GA at ultrasound and EFW percentile contributed significantly to the multivariable model (EFW percentile:  $\beta = 0.67$ ,  $P < 0.01$ ; GA at ultrasound:  $\beta = -0.20$ ,  $P < 0.01$ ). For the  $\Delta$ GA based on the SF and CB, the final models also included GA at ultrasound, EFW percentile and CPR, but only the EFW percentile was associated significantly (SF:  $\beta = 0.74$ ,  $P < 0.01$ ; CB:  $\beta = 0.56$ ,  $P = 0.04$ ). For POF and CLC, the final model consisted of GA at ultrasound and EFW percentile, but neither variable reached statistical significance. The adjusted  $R^2$  was 0.36 ( $P < 0.01$ ) for the whole scan, 0.14 ( $P = 0.03$ ) for SF, 0.11 ( $P = 0.03$ ) for POF and CLC, and 0.12 ( $P = 0.04$ ) for the CB. SES, fetal sex and CPR were not associated with the outcome. The interaction term (CPR\*sex) was not significant and did not improve any of the models.

**Table 1** Maternal, fetal and neonatal characteristics of 43 pregnancies with fetal growth restriction (FGR), overall and according to whether FGR was brain sparing

Characteristic	All FGR (n = 43)	Brain-sparing FGR (n = 13)	Non-brain-sparing FGR (n = 29)	P
Maternal age (years)	30.6 ± 4.7	31.1 ± 5.5	30.3 ± 4.4	0.62
Nulliparous	15 (34.9)	7 (53.8)	8 (27.6)	0.16
Maternal BMI (kg/m <sup>2</sup> )	24.5 ± 4.1	23.1 ± 3.3	25.1 ± 4.4	0.15
Caucasian ethnicity	27 (62.8)	8 (61.5)	19 (65.5)	0.38
Smoker	5 (11.6)	0 (0)	5 (17.2)	0.17
SES-WOA score	0.12 (0.00 to 0.23)	0.08 (−0.01 to 0.15)	0.13 (0.03 to 0.30)	0.16
Cardiovascular disease	3 (7.0)	0 (0)	3 (10.3)	0.54
Diabetes (Type 1 or 2)*	1 (2.3)	0 (0)	1 (3.4)	1.00
Thyroid disease	1 (2.3)	1 (7.7)	0 (0)	0.31
Autoimmune disease	4 (9.3)	1 (7.7)	2 (6.9)	1.00
Pre-eclampsia/HELLP syndrome†	15 (34.9)	8 (61.5)	7 (24.1)	0.04
Aspirin prophylaxis‡	8 (18.6)	1 (7.7)	6 (20.7)	0.40
Antihypertensive use	8 (18.6)	5 (38.5)	3 (10.3)	0.08
MgSO <sub>4</sub> administration	5 (11.6)	3 (23.1)	2 (6.9)	0.16
Antidepressant use	2 (4.7)	0 (0)	2 (6.9)	1.00
CCS administration	15 (34.9)	10 (76.9)	5 (17.2)	< 0.01
Female sex	26 (60.5)	4 (30.8)	22 (75.9)	0.01
GA at US (days)	190 (183–194)	193 (182–196)	189 (181–195)	0.51
HC (mm)	237.5 (224.5–246.7)	235.3 (224.6–245.3)	237.5 (221.5–247.0)	0.92
HC percentile	4.1 (0.6–16.4)	2.4 (0.05–12.7)	4.3 (1.1–15.3)	0.24
TCD (mm)	30.3 (27.8–31.5)	29.5 (28.6–31.4)	30.9 (26.3–31.5)	0.76
TCD percentile	33.6 (8.1–53.7)	12.0 (2.8–48.2)	39.9 (16.7–62.5)	0.09
AC (mm)	200.9 (184.1–214.4)	199.8 (183.1–205.0)	200.9 (184.4–217.6)	0.36
AC percentile	2.3 (0.2–6.5)	0.7 (0.0–1.6)	4.1 (0.3–8.3)	< 0.01
FL (mm)	44.6 (39.0–46.6)	42.1 (37.2–45.8)	45.1 (39.8–48.0)	0.20
FL percentile	0.7 (0.0–4.2)	0.0 (0.0–1.0)	1.8 (0.2–11.4)	0.01
EFW (g)	712 ± 213	660 ± 239	780 ± 309	0.40
EFW percentile	3.3 (0.5–6.3)	0.3 (0.1–2.2)	5.3 (1.1–7.9)	< 0.01
UA-PI	1.3 (1.2–1.6)	1.7 (1.5–2.1)	1.2 (1.1–1.3)	< 0.01
UA-PI percentile	81.0 (63.7–96.2)	99.4 (94.1–100.0)	74.6 (51.8–82.9)	< 0.01
MCA-PI	1.8 ± 0.5	1.5 ± 0.4	2.0 ± 0.4	< 0.01
MCA-PI percentile	17.4 (3.2–47.0)	1.5 (0.05–16.2)	25.2 (10.6–67.0)	< 0.01
CPR	1.4 ± 0.5	0.9 ± 0.3	1.6 ± 0.5	< 0.01
GA at birth (weeks)	37.0 (31.3–37.3)	31.3 (29.2–33.0)	37.1 (36.5–37.9)	< 0.01
Birth weight (g)	1486 (995–2262)	1000 (848–1110)	2120 (1273–2435)	< 0.01
Birth-weight percentile	0.7 (0.1–1.9)	0.1 (0.0–0.7)	1.1 (0.4–3.5)	< 0.01

Data are presented as mean ± SD, *n* (%) or median (interquartile range). One fetus in aggregated dataset developed brain-sparing FGR between two three-dimensional ultrasound scans and was excluded from brain-sparing and non-brain-sparing comparison. \*Including gestational diabetes mellitus in current pregnancy. †In current pregnancy. ‡In current pregnancy. AC, abdominal circumference; BMI, body mass index; CCS, corticosteroids; CPR, cerebropoplacental ratio; EFW, estimated fetal weight; FL, femur length; GA, gestational age; HC, head circumference; MCA, middle cerebral artery; MgSO<sub>4</sub>, magnesium sulfate; PI, pulsatility index; SES-WOA, socioeconomic status score based on financial wealth, education level and recent employment history of a household in a certain neighborhood; TCD, transcerebellar diameter; UA, umbilical artery; US, ultrasound.

**Table 2** Mean difference (Δ) between estimated and actual gestational age (GA) based on three-dimensional (3D) ultrasound volumes in 43 patients with fetal growth restriction (FGR), overall and according to whether FGR was brain sparing

3D ultrasound parameter	All FGR (n = 43)	P*	Brain-sparing FGR (n = 13)	Non-brain-sparing FGR (n = 29)	P
Whole scan (ΔGA (days))	−4.6 (−9.8 to −1.0)	< 0.001	−6.3 (−10.9 to −2.3)	−4.1 (−9.3 to −0.6)	0.30
Sylvian fissure (ΔGA (days))	−4.9 (−9.0 to −1.2)	< 0.001	−6.3 (−10.8 to −1.6)	−4.7 (−9.0 to −1.1)	0.56
Parieto-occipital fissure and calcarine sulcus (ΔGA (days))	−5.4 (−7.4 to −1.7)	< 0.001	−5.5 (−9.2 to −2.0)	−4.9 (−7.3 to 0.0)	0.47
Cerebellum (ΔGA (days))	−3.2 (−6.8 to 0.3)	< 0.001	−5.2 (−7.2 to −0.5)	−2.9 (−7.3 to −0.2)	0.82

Data are presented as median (interquartile range). One fetus in aggregated dataset developed brain-sparing FGR between two 3D ultrasound scans and was excluded from brain-sparing and non-brain-sparing comparison. \*Wilcoxon signed-rank test was used to compare estimated GA in days with actual GA at time of ultrasound.

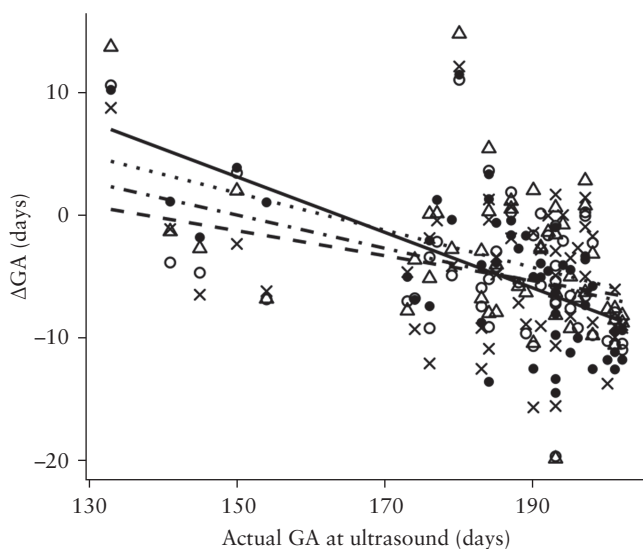


**Figure 2** Graph showing mean difference ( $\Delta$ ) between estimated and actual gestational age (GA) based on three-dimensional ultrasound volumes *vs* actual GA at ultrasound in 43 patients with fetal growth restriction. Formulae for lines of best fit: cerebellum ( $\bullet\cdot\Delta\cdot\cdot$ ),  $y = -0.12x + 18.55$ ; parieto-occipital fissure and calcarine sulcus ( $\cdot\cdot\circ\cdot\cdot$ ),  $y = -0.11x + 15.8$ ; sylvian fissure ( $\cdot\cdot\times\cdot\cdot$ ),  $y = -0.06x + 5.84$ ; and whole volume ( $\bullet\bullet\bullet$ ),  $y = -0.22x + 35.37$ .

### Neonatal outcomes

All 43 cases were liveborn at a median GA of 37.0 (IQR, 31.3–37.3) weeks, with a birth weight (BW) of 1486 (IQR, 995–2262) g. The brain-sparing FGR group were delivered at a significantly lower median GA of 31.3 (IQR, 29.2–33.0) weeks, with a median BW of 1000 (IQR, 848–1110) g compared with 37.1 (IQR, 36.5–37.9) weeks and 2120 (IQR, 1273–2435) g, respectively, in the non-brain-sparing FGR group (Table 1). Of the 43 liveborn neonates, 17 were admitted to the NICU because of delivery before 32.0 weeks. In eight neonates, either perinatal death or neurological or respiratory complications occurred. One case involved intrapartum death prior to NICU admission. Two neonates had neurological complications and five suffered from respiratory complications, one of which died during the NICU stay. More delayed antenatal brain maturation was seen in the more severe outcomes, but no statistically significant association was reached (Table 3).

### Logistic regression analysis of neonatal outcomes

We used logistic regression models for binary outcomes to assess the association between neonatal outcomes and GA at birth, BW and sex and the addition of  $\Delta$ GA. The model did not significantly improve by adding  $\Delta$ GA for NICU admission, combined neonatal morbidity and mortality or any respiratory complication. Since only two cases of perinatal death and neurological complications were included, it was not possible to build a model for these outcomes.

**Table 3** Association of binary perinatal outcomes with mean difference ( $\Delta$ ) between estimated and actual gestational age (GA) based on three-dimensional (3D) ultrasound volumes in 43 patients with fetal growth restriction

3D ultrasound parameter	Complications during NICU admission*			
	Perinatal death		NICU admission	
	Yes (n=2)†	No (n=41)	Yes (n=17)	No (n=25)
Whole scan ( $\Delta$ GA (days))	-10.4	-4.1 (-9.3 to -0.8)	-6.3 (-12.1 to -2.3)	-3.9 (-8.3 to 0.3)
Sylvian fissure ( $\Delta$ GA (days))	-11.4	-4.7 (-8.9 to -1.1)	-6.5 (-10.8 to -2.6)	-2.8 (-8.6 to -0.2)
Parieto-occipital fissure and calcarine sulcus ( $\Delta$ GA (days))	-8.2	-5.2 (-7.2 to -1.3)	-5.9 (-8.3 to -3.2)	-4.1 (-6.9 to 0.2)
Cerebellum ( $\Delta$ GA (days))	-6.7	-2.9 (-6.8 to 0.4)	-6.3 (-8.0 to -2.2)	-2.6 (-6.5 to 0.6)
			Combined neonatal morbidity and mortality	
			Yes (n=7)	No (n=9)
			-8.8 (-12.5 to -6.3)	-5.0 (-9.9 to -0.8)
			-9.2 (-12.5 to -6.3)	-3.4 (-8.7 to -0.1)
			-7.2 (-9.8 to -5.9)	-4.2 (-7.9 to -1.3)
			-4.6	-4.6
			Neurological complication	
			Yes (n=2)†	No (n=14)
			-9.9	-6.0 (-12.5 to -1.6)
			-10.0	-5.8 (-10.7 to -1.7)
			-7.8	-6.3 (-7.9 to -2.1)
			Respiratory complication	
			Yes (n=5)	No (n=11)
			-8.8 (-12.1 to -5.2)	-5.8 (-12.5 to -1.0)
			-9.2 (-13.1 to -6.8)	-5.0 (-10.6 to -1.5)
			-7.4 (-10.0 to -6.5)	-4.7 (-7.2 to -1.7)
			-6.8 (-8.7 to -4.6)	-3.2 (-8.0 to 0.6)

Data are presented as median or median (interquartile range). Combined neonatal morbidity and mortality encompassed neurological and/or respiratory complications or death in postnatal period until end of neonatal intensive care unit (NICU) admission. Neurological complications included perinatal asphyxia, intraventricular hemorrhage, posthemorrhagic ventricular dilation, cystic periventricular leukomalacia and stroke. Respiratory complications included need for mechanical ventilation, infant respiratory distress syndrome and bronchopulmonary dysplasia. \*One neonate died before NICU admission and another was born and admitted to NICU at a different perinatal center. †Only two cases included, so logistic regression analysis was not possible.

## DISCUSSION

Using a deep-learning-based automated method on 3D ultrasound volumes, we have shown delayed fetal gyrification in early-onset FGR before 29 weeks' gestation. The median estimated brain maturation delay based on the 3D ultrasound of the whole fetal brain was  $-4.6$  (IQR,  $-9.8$  to  $-1.0$ ) days. There was no significant difference in  $\Delta$ GA between fetuses with brain-sparing and non-brain-sparing FGR or between sexes. Interestingly, the observed delay in brain maturation was mostly associated with EFW percentile, even though all volume files were scaled up to the same size, indicating that prediction of maturation was independent of brain size. Furthermore, neonates with combined neonatal morbidity and mortality showed more delayed maturation, although this group also included those with the lowest EFW percentiles. However, the inclusion of delayed brain maturation as a variable did not improve the performance of any logistic regression model for neonatal complications.

We are the first group to describe brain maturation in early-onset FGR using automated analysis of the morphology of individual fissures on 3D ultrasound, enabling fast, accurate and reproducible fetal brain-age predictions. According to Wyburg *et al.*<sup>15</sup> the absolute error of the pipeline is 3.4, 5.0, 4.9 and 4.1 days, regardless of the direction, for the SF, POF, CLC and the whole brain, respectively. The magnitude of the error is similar to our findings, yet in our cohort a relatively consistent negative direction was observed.

### 3D ultrasound for gyrification in FGR

Gyrification on ultrasound is often estimated subjectively, by eye or by manually measuring the depth of sulci or attributing a score like Pistorius *et al.*<sup>13</sup> or Quarello *et al.*<sup>20</sup>. The Pistorius score has been assessed in early-onset FGR by Businelli *et al.*<sup>14</sup>, who described the opposite of our findings in growth-restricted fetuses, namely unchanged or even accelerated gyrification. It was hypothesized that stress promotes neurological maturation to prepare the fetus for preterm birth. When manually measuring the SF, POF and insula in early-onset FGR, only the right SF was slightly decreased, which could imply locally delayed brain maturation similar to our  $\Delta$ GA-SF results<sup>17</sup>. Another important hallmark in cortical maturation is insular development, which showed slower growth rates for smaller insulas on 3D ultrasound in early-onset FGR, also indicating a delay in brain maturation<sup>40</sup>.

### MRI for gyrification in FGR

Objective fetal brain-age prediction has been carried out using MRI. Parameters like gyrification, surface area, curvature and sulcal depth all correspond to specific GAs, but fetal MRI usually requires processing to correct for motion and is more time- and cost-intensive than ultrasound<sup>23,41</sup>. However, the mean absolute error for fetal brain-age prediction on MRI can be very

accurate, with an error of 0.875 days<sup>41</sup>. In contrast to this study, subjective assessment of brain maturation, classifying gyrification into eight GA-specific gyrus and sulcus formation stages on MRI in FGR fetuses, showed no differences<sup>42</sup>. A study by Yehuda *et al.*<sup>19</sup> implementing automated assessment on MRI did show lower gyrification indices for FGR fetuses at 33 weeks, which is in line with our findings. Neonate MRI data for FGR published by Dubois *et al.*<sup>11</sup> also support our findings indicating delayed gyrification. On the other hand, Bremilla *et al.*<sup>43</sup> and Ramenghi *et al.*<sup>44</sup> did not find a difference in total maturation score, which combines myelination, cortical folding, germinal matrix distribution and glial cell migration patterns, between FGR and appropriate-for-gestational-age neonates.

### Potential influencing factors

Interestingly, there was no effect of fetal sex and SES on  $\Delta$ GA in this study. There is a lot of heterogeneity regarding the role of sex. Some studies show that women have increased and more complex gyrification, whereas other studies suggest that men have increased surface area and gyrification indices<sup>45–47</sup>. Our entire cohort consisted of 60.5% female fetuses, and no significant differences in brain-maturation delay were observed (Table S1). The algorithm was trained on data from both sexes, potentially enabling it to account for sex-related differences. Lower SES has been associated with decreased cortical volumes and gyrification indices, however, in this study no effect was observed. This is potentially owing to the limited variability in our cohort or to other factors having a stronger influence on the maturation data<sup>48</sup>.

### Strengths and limitations

This was a prospective study and analysis of fetal brain age was done blinded to actual GA and clinical outcomes of the cohort. The automated pipeline was based on a large, healthy, international cohort and five-fold cross-validated. The 3D volume collection is part of standard care, minimizing bias.

However, there were some limitations including significant differences in baseline characteristics. Only four female fetuses had brain-sparing FGR, representing 30.8% of this group, whereas 75.9% of the non-brain-sparing FGR group were female. Nevertheless, in the linear regression analysis, neither fetal sex, CPR nor the interaction term CPR\*sex emerged as a significant covariate for delayed brain maturation. Another significant difference included corticosteroid administration, which is a logical consequence since brain-sparing FGR is more severe, leading to anticipated preterm birth and the administration of corticosteroids. In a larger cohort it would be valuable to investigate the effect of corticosteroids on brain maturation, since there is evidence for long-term physiological effects of antenatal corticosteroids, particularly on the fetal brain<sup>49,50</sup>. Our statistically significant results should be interpreted with

caution owing to the risk of a Type-I error. The limited sample size further restricted the number of variables that could be included in our multivariable model (e.g. maternal smoking) and caused the lack of power to build a model for perinatal death and neurological complications<sup>51–54</sup>. Additionally, CPR was used to define brain-sparing FGR, but this is an operator-dependent and dynamic measure, which might capture a transient state, whereas brain maturation is a more chronic adaptation to the *in-utero* environment<sup>55</sup>. Therefore, the lack of association may be due to the temporal mismatch. Although image acquisition was standardized and performed by experienced sonographers, some degree of interoperator variability cannot be entirely excluded.

Lastly, as the deep-learning model was trained and evaluated on external data, there is a risk that the observed differences reflect a domain shift rather than true biological variation. Moreover, a negative  $\Delta$ GA was considered indicative of delayed brain maturation, but this may also reflect normal phenotypic variation between groups in the absence of a clinical gold standard. Thus, evaluating the network performance on new populations is essential to assess its generalizability and potential broader clinical use.

### Clinical implications

This deep-learning-based automated method enables an objective analysis of gyrification, offering a potential alternative to manual scoring. Although this study focused on group-level comparisons, the model generates an estimated brain age for each fetus. The difference between estimated and actual age may be used to detect delayed maturation at the individual level, supporting future clinical application. This model could help to assess whether brain development is progressing as expected, since delayed cortical folding during gestation might be an early marker for impaired neurodevelopment later in life<sup>11,56</sup>. The method could aid in identifying fetuses with early-onset FGR at risk for adverse neurodevelopmental outcomes, allowing for a more tailored prognosis. On a global scale, reliable assessment of fetal growth is the first step before brain maturation can be evaluated, as brain-age prediction alone appears to be younger than the actual GA in early-onset FGR. Ultrasound-based deep-learning approaches may therefore offer a scalable and globally accessible solution to combine fetal growth and brain maturation assessment, paving the way for the earlier identification of neurodevelopmental risk and more personalized prenatal care.

### Conclusions

In this study we have illustrated delayed fetal brain maturation in early-onset FGR fetuses before 29 weeks' gestation using a 3D ultrasound deep-learning model. These findings highlight the potential role of this artificial intelligence methodology in the assessment of fetal brain maturation.

### ACKNOWLEDGMENTS

We thank GE Healthcare (Zipf, Austria) for offering an executable to enable the sharing of our volume files with the Oxford Machine Learning in Neuroimaging Laboratory, Department of Computer Science Oxford University, Oxford, UK.

### REFERENCES

- Dudink I, Hüppi PS, Sizonenko SV, et al. Altered trajectory of neurodevelopment associated with fetal growth restriction. *Exp Neurol*. 2022;347:113885.
- Malhotra A, Ditchfield M, Fahey MC, et al. Detection and assessment of brain injury in the growth-restricted fetus and neonate. *Pediatr Res*. 2017;82(2):184–193.
- Miller SL, Hüppi PS, Mallard C. The consequences of fetal growth restriction on brain structure and neurodevelopmental outcome. *J Physiol*. 2016;594(4):807–823.
- Fleiss B, Wong F, Brownfoot F, et al. Knowledge gaps and emerging research areas in intrauterine growth restriction-associated brain injury. *Front Endocrinol (Lausanne)*. 2019;10:188.
- Sun L. The update of fetal growth restriction associated with biomarkers. *Matern Fetal Med*. 2022;4(3):210–217.
- Dall'Asta A, Brunelli V, Prefumo F, Frusca T, Lees CC. Early onset fetal growth restriction. *Matern Health Neonatol Perinatol*. 2017;3:2. <https://doi.org/10.1186/s40748-016-0041-x>.
- Baschat AA. Neurodevelopment following fetal growth restriction and its relationship with antepartum parameters of placental dysfunction. *Ultrasound Obstet Gynecol*. 2011;37(5):501–514.
- Bruin C, Damhuis S, Gordijn S, Ganzevoort W. Evaluation and management of suspected fetal growth restriction. *Obstet Gynecol Clin North Am*. 2021;48(2):371–385.
- Cohen E, Baerts W, Caicedo Dorado A, Nauelaers G, Van Bel F, Lemmers PMA. Cerebrovascular autoregulation in preterm fetal growth restricted neonates. *Arch Dis Child Fetal Neonatal Ed*. 2019;104(5):F467–F472.
- Cohen E, Baerts W, Alderliesten T, Derks J, Lemmers P, Van BF. Growth restriction and gender influence cerebral oxygenation in preterm neonates. *Arch Dis Child Fetal Neonatal Ed*. 2016;101(2):F156–F161.
- Dubois J, Benders M, Borradori-Tolsa C, et al. Primary cortical folding in the human newborn: An early marker of later functional development. *Brain*. 2008;131(8):2028–2041.
- Namburete AIL, Stebbing RV, Kemp B, Yaqub M, Papageorgiou AT, Alison NJ. Learning-based prediction of gestational age from ultrasound images of the fetal brain. *Med Image Anal*. 2015;21(1):72–86.
- Pistorius LR, Stoutenbeek P, Groenendaal F, et al. Grade and symmetry of normal fetal cortical development: a longitudinal two- and three-dimensional ultrasound study. *Ultrasound Obstet Gynecol*. 2010;36(6):700–708.
- Businelli C, de Wit C, Visser GHA, Pistorius LR. Ultrasound evaluation of cortical brain development in fetuses with intrauterine growth restriction. *J Matern Fetal Neonatal Med*. 2015;28(11):1302–1307.
- Wyburd MK, Hesse LS, Aliasi M, et al. Assessment of Regional Cortical Development Through Fissure Based Gestational Age Estimation in 3D Fetal Ultrasound. *Lecture Notes in Computer Science (Including Subseries Lecture Notes in Artificial Intelligence and Lecture Notes in Bioinformatics)*. LNCS. Vol 12959. Springer Science and Business Media Deutschland GmbH; 2021:242–252.
- Pooh RK, Machida M, Nakamura T, et al. Increased Sylvian fissure angle as early sonographic sign of malformation of cortical development. *Ultrasound Obstet Gynecol*. 2019;54(2):199–206.
- Husen SC, Koning IV, Go ATJI, et al. Three-dimensional ultrasound imaging of fetal brain fissures in the growth restricted fetus. *PLoS One*. 2019;14(5):e0217538.
- Yehuda B, Rabinowich A, Link-Sourani D, et al. Automatic quantification of normal brain gyrification patterns and changes in fetuses with polymicrogyria and lissencephaly based on MRI. *Am J Neuroradiol*. 2023;44(12):1432–1439.
- Yehuda B, Rabinowich A, Zilberman A, et al. Reduced gyrification in fetal growth restriction with prenatal magnetic resonance images. *Cereb Cortex*. 2024;34(6):bhae250.
- Quarello E, Stirnemann J, Ville Y, Guibaud L. Assessment of fetal Sylvian fissure opercularization between 22 and 32 weeks: a subjective approach. *Ultrasound Obstet Gynecol*. 2008;32(1):44–49.
- Rodriguez-Sibaja MJ, Villar J, Ohuma EO, et al. Fetal cerebellar growth and Sylvian fissure maturation: international standards from Fetal Growth Longitudinal Study of INTERGROWTH-21st Project. *Ultrasound Obstet Gynecol*. 2021;57(4):614–623.
- Chen X, Li SL, Luo GY, et al. Ultrasonographic characteristics of cortical sulcus development in the human fetus between 18 and 41 Weeks of gestation. *Chin Med J (Engl)*. 2017;130(8):920–928.
- Bekker MN, van Vugt JM. The role of magnetic resonance imaging in prenatal diagnosis of fetal anomalies. *Eur J Obstet Gynecol Reprod Biol*. 2001;96(2):173–178.
- Namburete AIL, Papież BW, Fernandes M, et al. Normative spatiotemporal fetal brain maturation with satisfactory development at 2 years. *Nature*. 2023;623(7985):106–114.
- Hesse LS, Aliasi M, Moser F, et al. Subcortical segmentation of the fetal brain in 3D ultrasound using deep learning. *Neuroimage*. 2022;254:119117.
- Hadlock FP, Harrist RB, Sharman RS, Deter RL, Park SK. Estimation of fetal weight with the use of head, body, and femur measurements—a prospective study. *Am J Obstet Gynecol*. 1985;151(3):333–337.

27. Monteith C, Flood K, Pinnamaneni R, et al. An abnormal cerebroplacental ratio (CPR) is predictive of early childhood delayed neurodevelopment in the setting of fetal growth restriction. *Am J Obstet Gynecol*. 2019;221(3):273.e1-273.e9.
28. Malinger G, Paladini D, Haratz KK, Monteagudo A, Pilu GL, Timor-Tritsch IE. ISUOG Practice Guidelines (updated): sonographic examination of the fetal central nervous system. Part 1: performance of screening examination and indications for targeted neurosonography. *Ultrasound Obstet Gynecol*. 2020;56(3):476-484.
29. Paladini D, Malinger G, Birnbaum R, et al. ISUOG Practice Guidelines (updated): sonographic examination of the fetal central nervous system. Part 2: performance of targeted neurosonography. *Ultrasound Obstet Gynecol*. 2021;57(4):661-671.
30. Papageorgiou AT, Ohuma EO, Altman DG, et al. International standards for fetal growth based on serial ultrasound measurements: the Fetal Growth Longitudinal Study of the INTERGROWTH-21st Project. *Lancet*. 2014;384(9946):869-879.
31. Moser F, Huang R, Papież BW, Namburete AIL. BEAN: brain extraction and alignment network for 3D fetal neurosonography. *Neuroimage*. 2022;258:119341.
32. IBM Corp. Released *IBM SPSS Statistics for Windows, Version 27.0*. IBM Corp; 2020.
33. R Core Team. A Language and Environment for Statistical Computing. *Foundation for Statistical Computing*. Preprint posted online 2024.
34. Ghasemi A, Zahediasl S. Normality tests for statistical analysis: a guide for non-statisticians. *Int J Endocrinol Metab*. 2012;10(2):486-489.
35. [Volksgesondheidszorg.info](https://www.vzinfo.nl/vroeggeboorte-ondergewicht-enof-groeivertraging). Zorg bij vroeggeboorte, ondergewicht en/of groeivertraging. <https://www.vzinfo.nl/vroeggeboorte-ondergewicht-enof-groeivertraging/zoorg>.
36. Ward RM, Beachy JC. Neonatal complications following preterm birth. *BJOG* 2003;110(Suppl 20):8-16.
37. Gardella B, Dominoni M, Scatigno AL, et al. What is known about neuroplacentology in fetal growth restriction and in preterm infants: a narrative review of literature. *Front Endocrinol (Lausanne)*. 2022;13:936171.
38. Parmentier CEJ, El Bakkali L, Verhagen EA, et al. Brain MRI injury patterns across gestational age among preterm infants with perinatal asphyxia. *Neonatology*. 2024;121(5):616-626.
39. Arts K, van Gaalen R, van der Lan J, et al. Berekenwijze sociaal economische status scores. <https://www.cbs.nl/nl-nl/maatwerk/2021/45/berekenwijze-ses-score-per-wijk-buurt>
40. Xue J, Xue J, Ru Y, Zhang G, Yin H, Liu D. Ultrasound assessment of insular development in adequate-for-gestational-age fetuses and fetuses with early-onset fetal growth restriction using 3D-ICRV technology. *Front Med (Lausanne)*. 2024;11:1393115.
41. Hong J, Yun HJ, Park G, et al. Optimal method for fetal brain age prediction using multiplanar slices from structural magnetic resonance imaging. *Front Neurosci*. 2021;15:714252.
42. Abel S, Takagi K, Yamamoto T, et al. Assessment of cortical gyrus and sulcus formation using magnetic resonance images in small-for-gestational-age fetuses. *Prenat Diagn*. 2004;24(5):333-338.
43. Brembilla G, Righini A, Scelsa B, et al. Neuroimaging and neurodevelopmental outcome after early fetal growth restriction: NEUROPROJECT-FGR. *Pediatr Res*. 2021;90(4):869-875. <https://pubmed.ncbi.nlm.nih.gov/33469173/>
44. Ramenghi LA, Martinelli A, De Carli A, et al. Cerebral maturation in IUGR and appropriate for gestational age preterm babies. *Reprod Sci*. 2011;18(5):469-475.
45. Kaczurkin AN, Raznahan A, Satterthwaite TD. Sex differences in the developing brain: insights from multimodal neuroimaging. *Neuropsychopharmacology*. 2019;44(1):71-85.
46. Luders E, Narr KL, Thompson PM, et al. Gender differences in cortical complexity. *Nat Neurosci*. 2004;7(8):799-800.
47. Luders E, Gaser C, Spencer D, et al. Cortical gyrification in women and men and the (missing) link to prenatal androgens. *Eur J Neurosci*. 2024;60(2):3995-4003.
48. Lu YC, Kapse K, Andersen N, et al. Association between socioeconomic status and in utero fetal brain development. *JAMA Netw Open*. 2021;4(3):e213526.
49. Chang YP. Evidence for adverse effect of perinatal glucocorticoid use on the developing brain. *Korean J Pediatr*. 2014;57(3):101-109.
50. Matthews SG. Antenatal glucocorticoids and programming of the developing CNS. *Pediatr Res*. 2000;47(3):291-300.
51. Heinze G, Schemper M. A solution to the problem of separation in logistic regression. *Stat Med*. 2002;21(16):2409-2419.
52. Peduzzi P, Concato J, Kemper E, Holford TR, Feinstein AR. A simulation study of the number of events per variable in logistic regression analysis. *J Clin Epidemiol*. 1996;49(12):1373-1379.
53. Banerjee A, Chitnis UB, Jadhav SL, Bhawalkar JS, Chaudhury S. Hypothesis testing, type I and type II errors. *Ind Psychiatry J*. 2009;18(2):127.
54. Ekblad MO. Association of smoking during pregnancy with compromised brain development in offspring. *JAMA Netw Open*. 2022;5(8):E2224714.
55. Yagel S, Cohen SM, Valsky DV. The cerebroplacental ratio: a useful marker but should it be a screening test? *Ultrasound Obstet Gynecol*. 2025;65(5):541-545.
56. Lefèvre J, Germanaud D, Dubois J, et al. Are developmental trajectories of cortical folding comparable between cross-sectional datasets of fetuses and preterm newborns? *Cerebral Cortex*. 2016;26(7):3023-3035.

## SUPPORTING INFORMATION ON THE INTERNET

The following supporting information may be found in the online version of this article:



**Table S1** Mean difference ( $\Delta$ ) between estimated and actual gestational age (GA) based on three-dimensional (3D) ultrasound volumes in 43 patients with fetal growth restriction, according to fetal sex.

**Figure S1** Graph showing correlation between total brain volume and estimated gestational age (GA) based on three-dimensional ultrasound whole-brain morphology in 43 patients with fetal growth restriction.